

Original Research Article

Platelet-leukocyte-rich plasma (L-PRP) prevents the collagen III degradation and impairs the bone matrix development in artificial defect of rabbit calvaria, associated with suppression of the immunohistochemical expression of MMP-2 and MMP-9

Anselmo Gabriel Wruck Garcia¹
Rafaela Scariot¹
Melissa Rodrigues de Araujo¹
Emanuelle Juliana Cunha¹
Jaqueline Muller Henn²
João Ricardo de Almeida Grossi¹
Tatiana Miranda Deliberador¹
João Cesar Zielak¹
Allan Fernando Giovanini¹

Corresponding author:

Allan Fernando Giovanini
Universidade Positivo
Rua Pedro Viriato Parigot de Souza, n. 5.300
CEP 81280-330 – Curitiba – PR – Brasil
E-mail: afgiovanini@gmail.com

¹ Master Program in Clinical Dentistry, Positivo University – Curitiba – PR – Brazil.

² School of Dentistry, Positivo University – Curitiba – PR – Brazil.

Received for publication: August 12, 2014. Accepted for publication: September 15, 2014.

Keywords:

bone regeneration;
metalloproteinases;
collagen III; platelet-
rich plasma.

Abstract

Introduction and Objective: Because L-PRP constitutes an important source of growth factor that is associated with osteogenesis and fibrogenesis, the aim of this study was to evaluate the effect of L-PRP on the presence of collagen III and MMP-2 and MMP-9, while comparing these results by means of a histomorphometric analysis of bone matrix and fibrous deposition on bone repair. **Material and methods:** Four bone defects of 8 × 2 mm were created on the calvaria of 21 rabbits. The surgical defects were treated with either particulate autograft, particulate autograft mixed with L-PRP, or L-PRP alone. Animals were euthanized at 2, 4, and 6 weeks postoperative. Histomorphometric and immunohistochemical analyses were performed to assess repair time, as well as the expression of

collagen III and MMPs. **Results:** In contrast to the results of the L-PRP-free groups, the histomorphometric results of the L-PRP groups demonstrated intense fibrotic deposition along with hindered bone matrix deposition. These results coincided with the larger occurrence of diffuse collagen III deposition and the scarce presence of MMP-2 and -9 spread among the fibrous tissue. **Conclusion:** Thus, the results suggest that L-PRP not only induces an intense fibrosis rich in collagen III, which is not degraded, but also suppresses MMP-2 and -9 expressions, mimicking a similar pathological event as that of a cleft-palate or cranial suture.

Introduction

Leukocyte-platelet-rich plasma (L-PRP) is a blood-derived portion composed of high concentrations of platelets and white cells, and it has been applied as autogenous biomaterial in bone repair [13]. The reason for its use is the higher number of platelets, which is an important source of growth factors, such TGF- β 1, that hypothetically possess a stimulating effect on regulation and differentiation in mesenchymal tissue repair [10].

Regardless of this justification, some studies have demonstrated negative action of L-PRP on osteogenesis [1, 10, 16, 18] at the same time that fibrosis is produced [5, 6] generating conflict about the real clinical effect of L-PRP in bone reparative sites.

Fibrosis generally occurs due to dysregulation of mechanisms that control the usual extracellular matrix (ECM) turnover [11]. It is generally orchestrated by higher levels of TGF- β 1 [14], simultaneously inhibiting ECM degradation by suppressing metalloproteinase, especially MMP-2 and MMP-9 [20].

It is noteworthy that both TGF- β 1 and MMP-2 and -9 are synthesized by activated platelets during their aggregation [9]. In addition, osteoblasts also express MMPs, whose presence seems to be crucial in embryological bone development, because they are required for the formation of secondary ossification during cranial and palate bone formation [2].

We hypothesized that L-PRP could alter the immunoexpression of MMP-2 and -9 and alters the ratio between fibrotic conditions and osteogenesis. Thus, the aim of this study was to verify the immunolocalization of MMP-2 and -9 and collagen III in rabbit calvarium bone defects treated with and without L-PRP insertion.

Material and methods

In this study, 21 New Zealand female rabbits, ranging in age from 350 to 370 days, weighing 2.75 to 4.60 kg, with no previous disease, were used following a protocol approved by the Institutional Animal Care and Use Committee of Positivo University (Curitiba, PR, Brazil).

L-PRP fabrication and its quantification

A 15 ml sample of autologous blood was collected from each animal through cannulation of the ear vein into a syringe containing 1.48 ml of 10% sodium citrate. The blood samples were centrifuged at $200 \times g$ for 20 min at room temperature to separate the plasma containing the platelets from the red cells (Beckman J-6M Induction Drive Centrifuge; Beckman Instruments Inc., Palo Alto, CA, USA). The plasma fraction was removed from the top of the supernatant. The remaining fractions were centrifuged again at room temperature for 10 min at $400 \times g$ to separate the platelets. The platelet-poor plasma was removed from the upper level of the supernatant, leaving the L-PRP and buffy coat (1.0 ml), which were re-suspended and activated with a mixture of 10% calcium chloride (0.05 ml/ml of L-PRP). They were added to the previously prepared L-PRP and mixed for approximately 1 min until they formed a gel.

The platelets and leukocytes in the L-PRP were measured after centrifugation using a Coulter STKS hematology-counting machine (Beckman-Coulter, Chicago, IL, USA). An average of 2.5×10^6 (Standard deviation of 1.6×10^6)₊ platelets/ μ L was achieved, whereas initial values accounted for approximately 3.0×10^5 (1.1×10^5) platelets/ μ L. Simultaneously, an average of 4.3×10^4 (0.8×10^4) leukocytes/ μ L was measured in the L-PRP, while the initial blood values were 9.3×10^3 (0.10×10^3) leukocytes/ μ L.

Surgical procedure

The rabbits were anesthetized by an intramuscular injection of xylazine (5 mg/kg) and ketamine (70 mg/kg). The surgical region was shaved and aseptically prepared. A 5 cm midline dermo periosteal incision was made to expose the calvarial surface. Four circular defects of 8 mm in diameter \times 2 mm in depth were created with a trephine (Biomedic Research Instruments Inc., Silver Springs, MD, USA) under abundant saline solution irrigation.

Bone fragments removed from the calvaria defects were used for particulate autograft. One defect was filled with 0.01 ml of autograft (group I), another received 0.01 ml of autograft associated with 100 μ L of L-PRP (group II), and a third was filled with 100 μ L of L-PRP alone (group III). For the control defects (sham), no grafting material was inserted (group IV). Each animal received a prophylactic intramuscular injection of 24,000 IU of penicillin G-benzathine.

Euthanasia procedure and tissue processing

The animals were euthanized with an overdose (10 mg/kg) of intravenous sodium thiopental at 2, 4 and 6 weeks post-surgery ($n = 7$ animals/period). The calvaria of the animals were removed in blocks, using an inverted cone bur. The calvaria were fixed in 10% buffered formalin for 48 h and decalcified in 20% formic acid and sodium citrate for 7 days. The specimens were processed and embedded in paraffin. Serial histological sections of 3 μ m perpendicular to the mid-sagittal suture were performed and stained with Masson's trichrome to enable histomorphological and histomorphometric evaluation.

Immunohistochemistry processing

For each specimen, 3 μ m thicknesses were deparaffinized and subjected to antigen retrieval in 1% pepsin solution (pH 1.8) for 60 min at 37°C. The slides containing the fragments were immersed in 3% hydrogen peroxide for 30 min followed by incubation with 1% phosphate-buffered saline (PBS; pH 7.4). The sections were incubated with the primary antibody anti-MMP-2 (Santa Cruz Biotechnology Inc., sc 146, Santa Cruz, CA, USA) with a dilution factor of 1:100, and anti-MMP-9 (Abcam, Cambridge, UK, ab 6285) with a dilution factor of 1:150,

overnight (18 h). The labeled streptavidin biotin antibody-binding detection system (Universal HRP Immunostaining Kit-Diagnostic Biosystem Universal HRP Immunostaining Kit; Diagnostic Biosystem, Foster City, CA, USA) was applied to detect the primary antibodies. The immune reaction was revealed with the diaminobenzidine-tetrachloride chromogen solution (Universal HRP Immunostaining Kit; Diagnostic Biosystem, Foster City, CA, USA) and counterstained with Harris-hematoxylin. A negative control was performed using rabbit polyclonal IgG isotype (2 μ g/ml; Abcam, Cambridge, UK, ab 27472) for 10 min at room temperature as a primary antibody.

Image analysis

The images of the histological and immunohistochemistry sections were captured by a digital camera (SDC-310; Samsung, Kyungki-Do, South Korea) coupled with a light microscope (ZEISS, Germany) with an original magnification of \times 100. Each digital image was gathered and preserved with 300 dpi resolution.

All measurements were made using the software ImageJ (National Institute of Health, Bethesda, MD, USA). The perimeters of histological areas (bone matrix and fibrosis) were carefully traced, all areas were computed, and their values were transformed into percentage. At the same time, the percentage of positive MMP-2 and -9 were determined by automation, following the protocol established by Di Cataldo *et al.* [3].

Statistical analysis

Each parameter was evaluated within the monitoring period. An analysis of variance (Anova) was used to determine if there were significant differences among groups, followed by the Student-Newman-Keuls non-parametric test. A p value of less than .05 was considered to be statistically significant.

Results

Light microscopic analysis

Quantitative data of the histomorphometric analysis is given in table I. A summary report of histological characteristics is presented below.

Table I - Means (standard deviation - SD) of percentage of bone matrix and fibrous tissue found among the groups

		Autograft	L-PRP + Autograft	L-PRP	Sham
2 nd week	Bone matrix	53.20 (4.29)*	41.21 (4.12)*	2.79 (1.89)**	6.52 (2.13)**
	Fibrous tissue	41.46 (3.82)**	49.32 (5.36)**	83.06 (5.06)*	78.94 (4.04)*
4 th week	Bone matrix	71.22 (3.28)*	48.91 (2.10)**	7.28 (3.97)***	37.22 (4.39)**
	Fibrous tissue	16.67 (3.44)***	44.69 (3.93)*/**	78.71 (3.84)*	26.55 (3.11)**
6 th week	Bone matrix	84.74 (3.93)*	54.15 (3.28)**	12.98 (2.67)***	59.10 (4.35)**
	Fibrous tissue	06.67 (2.82)***	42.81 (4.41)*	69.47 (3.29)*	18.61 (4.09)**

For each line, values followed by the same superscript are statistically similar, $p > 0.05$

Medullary adipose area not accounted

Bone fragments grafted and surrounded by mesenchymal tissue were detected in group I and group II, but evident increase of *de novo* bone formation was observed in the L-PRP-free group, while the L-PRP group exhibited fibrosis. These histological features were similar to those of 4 and 6 weeks post-surgery. The histological frame in group III and group IV at 2 weeks post-surgery revealed fibrous tissue that compounded the body of defect. However, at 4 and 6 weeks post-surgery, failure of bone matrix development was present only in group III, while in group IV an evident new bone matrix formation was observed.

Immunohistochemical results

A quantitative data of the immunohistochemistry is given in table II. A summary report of the immunohistochemical characteristics found among groups is presented below.

Table II - Means (standard deviation - SD) of percentage of immunoexpression of Collagen III, MMP-2 and MMP-9 among the groups

Period	protein	Groups			
		Autograft	L-PRP + Autograft	L-PRP	Sham
2 nd week	Collagen III	5.06 (1.66)**	36.31 (2.04)*	47.29 (4.28)*	13.36 (2.81)**
	MMP2	42.13 (2.98)*	6.12 (1.04)**	2.61 (0.76)**	51.11 (3.57)*
	MMP9	36.81 (1.27)*	2.41 (0.36)**	1.99 (0.06)**	42.32 (2.16)*
4 th week	Collagen III	4.76 (0.98)*	34.88 (3.26)**	42.09 (2.27)***	7.12 (1.12)**
	MMP2	33.82 (2.14)*	3.19 (0.88)**	1.21 (0.14)**	31.18 (1.60)*
	MMP9	29.16 (2.07)*	1.81 (0.37)***	0.72 (0.19)***	21.11 (1.96)**
6 th week	Collagen III	3.26 (0.42)*	28.21 (2.43)**	37.93 (2.27)***	3.10 (0.35)**
	MMP2	18.61 (4.09)*	1.71 (0.01)**	0.87 (0.13)**	21.16 (1.28)*
	MMP9	14.72 (1.47)*	< 0.01	0.12 (0.02)**	17.57 (1.36)*

For each line, values followed by the same superscript are statistically similar, $p > 0.05$

Collagen III

All groups exhibited positivity to collagen III. At 2 weeks post-surgery, scarce and restricted positive fibers of collagen III were observed on the L-PRP-free groups (figure 1). This immunopositivity occurred especially surrounding the blood vessels, haversian canals, and areas represented by a common bone marrow ECM. In contrast, intense and diffuse deposition of collagen III was observed in the L-PRP groups in all time periods analyzed (figure 2).

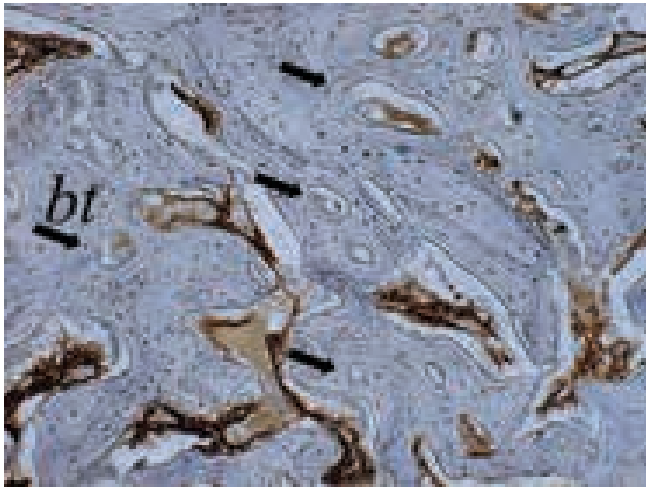


Figure 1 - Reveals the scarce immunopositivity of Collagen III (brownish color) surrounding the blood vessel in medullary area neoformed at 4th week post-surgery in L-PRP-free group associated to autograft (group I). Verify the intense presence of haversian bone deposition (bt) exhibiting well-defined osteon (arrow) (Original magnification $\times 100$)

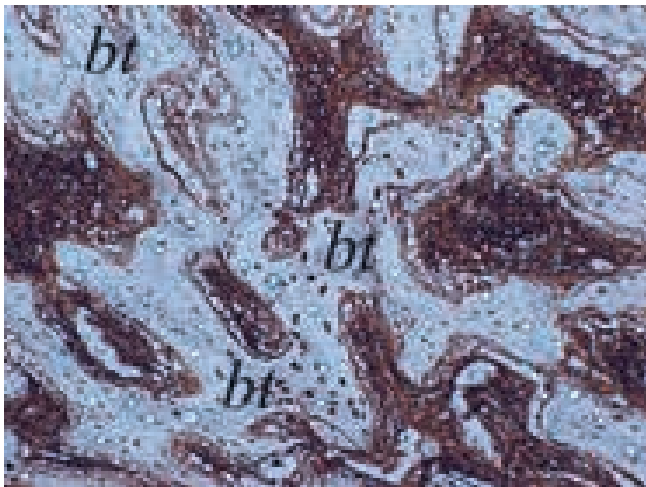


Figure 2 - Show the larger area composed by Collagen III (brownish color) among the thin bone trabeculae (bt) at 6th week post-surgery in group treated with L-PRP (group II) (Original magnification $\times 100$)

MMP-2

The percentage of positivity to MMP-2 was markedly higher in the L-PRP-free group. In this group, the immunopositivity was concentrated in the ECM or even surrounding the engrafted bone for group I (figure 3). In contrast, in groups II and III, few ECM areas exhibited positivity to MMP-2, and they were scarce and restricted to adjacencies on

the bone graft or concentrated peripherally to the host bone. A similar immunohistochemical pattern was observed at both 4 and 6 weeks post-surgery both in group II (figure 4) and group III.

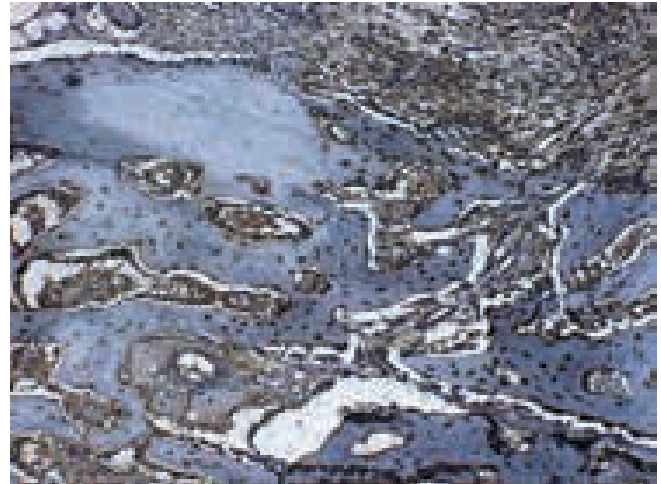


Figure 3 - Micrograph demonstrates the intense positivity for MMP-2 (brownish color) in the extracellular matrix and bone cells in group L-PRP-free (group I) at 4th week post-surgery (Original magnification $\times 100$)

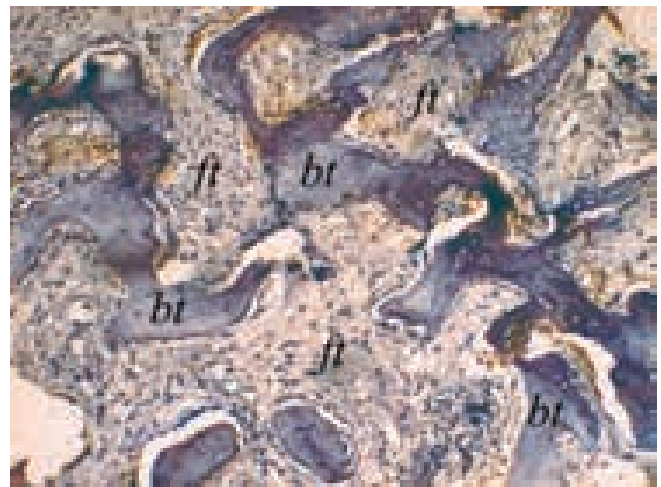


Figure 4 - Verify the scarce immunolabel for MMP-2 (brownish color) in peritrabecular area (bt) in the group treated with L-PRP (group II) at 4th week post-surgery. Verify the intense presence of fibrous tissue (ft) surrounding the thin bone trabeculae at 6th week post-surgery (Original magnification $\times 100$)

MMP-9

The investigation of immunolocalization of MMP-9 showed similar results to that of MMP-2. Despite all groups demonstrating positivity to

MMP-9, the group treated with L-PRP revealed scarce, or even a lack of, immunopositivity for metalloproteinase in all time periods analyzed. In contrast, in the L-PRP-free group, immunopositivity was remarkable, but its percentage decreased as the bone matrix was developed. The differences of immunohistochemical pattern can be seen in figure 5 (specimen treated with L-PRP [group II]) and figure 6 (control group [group IV])

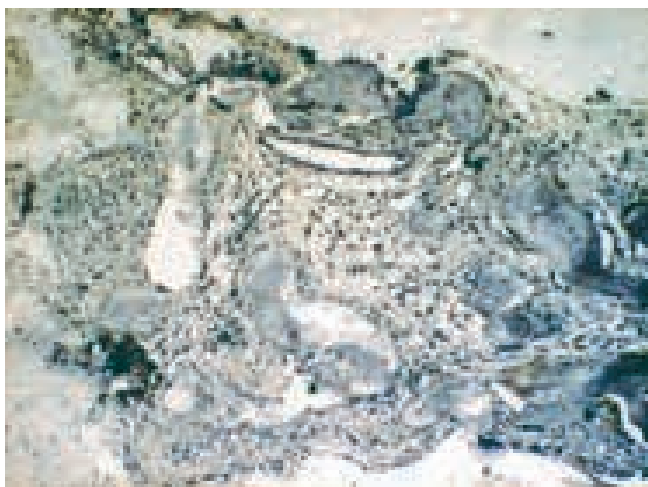


Figure 5 - Micrograph revealing absence of substantial immunostaining for MMP-9 (brownish color) in L-PRP group at 4th week post-surgery. Verify the intense presence of fibrous tissue (ft) among the particulate bone graft (bt) (Original magnification $\times 40$)



Figure 6 - Histological features demonstrating the immunolocalization of MMP-9 (brownish color) in L-PRP-free group at 4th week post-surgery (Original magnification $\times 100$)

Discussion

In this study, it was revealed that in calvaria treated with L-PRP, failure in bone matrix deposition

occurred simultaneously with an increase in histophenotype fibrotic conditions. These results also occurred simultaneously with maintained collagen III and the absence of the immunohistochemical expression of MMP-2 and -9.

The increase in collagen III is an event expected at earlier time periods in the L-PRP group, because platelets depend on this type of collagen for platelet aggregation and activation [5, 15]. However, the maintenance of collagen III seems to configure the fibrotic conditions and the subsequent negative effect of L-PRP in bone regeneration, because the presence of collagen III neither surrounds nor supports the adhesion of bone cells [22].

This fibrotic condition corroborates with other studies and may be attributed to changes in TGF- β . In this way, Giovanini *et al.* [7] demonstrated that L-PRP produced a cross-reaction between TGF- β 1 and Wnt10b osteo-protein, a fact that is commonly associated with the inhibition of osteoneogenesis and adipogenesis, but favoring fibrosis. In addition, Giovanini *et al.* [6] showed significant fibrosis rich in collagen III, the presence of α -smooth-actin+ cells, and higher levels of TGF- β associated with platelet-concentrated situations that are commonly found in pathological fibrotic conditions. These studies [6, 7] may also give support to results present herein, because the TGF- β 1 is a common platelet growth factor that also may modulate the suppression of MMP-2 and -9 and consequently impairs ECM degradation [20].

Our speculation is based on a study published by Risinger *et al.* [20] which revealed that exogenous TGF- β 1 inhibits MMP-2, and this mechanism seems to be connected to the presence of the integrity of the actin cytoskeleton induced by its own TGF- β 1. This conclusion was derived from the observation that forcing the disassembly of actin stress fibers caused the blocked ability of TGF- β 1 to suppress the upregulation of MMP-2, but in the opposite situation, these actin+ cells produce an increase in TGF- β 1 that in turn reduces MMP-2 expression.

In addition, the antagonistic expression between MMP-9 and TGF- β 1 seems to be a common event. However, despite MMP-2 and -9 sharing structural and catalytic similarities, the suppression pathways of MMP-9 via TGF- β 1 occur indirectly and differently from those of MMP-2. Using a cell culture of lymph reticular cells, Ogawa *et al.* [19] showed that the interaction between TGF- β 1 and its receptors produced biological events via the phosphorylation of SMADs that impairs the transcription of the nuclear factor KB (NF-KB) site, a locus that contains the -670/-591 bp that

corresponds to the MMP-9 promoter region. This event inhibits the transcription and expression of MMP-9, at the same time that it maintains the basal expression of TGF- β 1.

Thus, these results may help to explain the scarce immunohistochemical condition of MMP-2 and -9 and fibrotic development in reparative sites. In addition, the lack of MMP-2 and -9 may be indicative of a fundamental condition of the failure of bone matrix deposition, not only associated with suppressing collagen III degradation, but also associated with failure of bone matrix construction.

This proposition originates from the premises that MMPs are not only destructive enzymes but also active biomolecules that play roles in cell attachment, proliferation, and differentiation, [12] including in osteo-lineage cells [4, 21]. In this way, Mosig *et al.* [17] using the knockout MMP genes in mouse models, described how a lack of MMP-2 interrupted craniofacial skeleton development; these results are also corroborated by Demarchi *et al.* [2] who added that both MMP-2 and -9 are necessary for suture fusion, because these MMPs are responsible for secondary ossification on craniofacial defects.

In this study, we demonstrated that L-PRP could impair bone repair in craniofacial defects, because maintaining collagen III and suppressing MMP-2 and -9 mimics a usual etiology present not only in fibroproliferative conditions, but also in cleft-palate or suture development.

References

1. Choi BH, Im CJ, Huh JY, Suh JJ, Lee SH. Effect of platelet-rich plasma on bone regeneration in autogenous bone graft. *Int J Oral Maxillofac Surg.* 2004;33:56-9.
2. Demarchi ACO, Zambuzzi WF, Paiva KB, Silva-Valenzuela M, Nunes FD, Figueira RCS *et al.* Development of secondary palate requires strict regulation of ECM remodeling: sequential distribution of RECK, MMP-2, MMP-3, and MMP-9. *Cell Tissue Res.* 2010;340:61-9.
3. Di Cataldo S, Ficarra E, Acquaviva A, Macii E. Automated segmentation of tissue images for computerized IHC analysis. *Comput Methods Programs Biomed.* 2010;100:1-15.
4. Filanti C, Dickson GR, Di Martino D, Ulivi V, Sanguineti C, Romano P *et al.* The expression of metalloproteinase-2, -9, and -14 and of tissue inhibitors-1 and -2 is developmentally modulated during osteogenesis *in vitro*, the mature osteoblastic phenotype expressing metalloproteinase-14. *J Bone Miner Res.* 2000;15:2154-68.
5. Giovanini AF, Deliberador TM, Gonzaga CC, Oliveira Filho MA, Gohringer I, Kuczera J *et al.* Platelet-rich plasma diminishes calvarial bone repair associated with alterations in collagen matrix composition and elevated CD34+ cell prevalence. *Bone.* 2010;46:1597-603.
6. Giovanini AF, Gonzaga CC, Zielak JC, Deliberador TM, Kuczera J, Goringher I *et al.* Platelet-rich plasma (PRP) impairs the craniofacial bone repair associated with its elevated TGF-beta levels and modulates the co-expression between collagen III and alpha-smooth muscle actin. *J Orthop Res.* 2011;29:457-63.
7. Giovanini AF, Deliberador TM, Tannuri Nemeth JE, Crivellaro VR, Portela GS, Oliveira Filho MA *et al.* Leukocyte-platelet-rich plasma (L-PRP) impairs the osteoconductive capacity of the autograft associated to changes in the immunolocalization of TGF-beta1 and its co-expression with Wnt10b and CD34 cells. *J Craniomaxillofac Surg.* 2013;41(7): e180-6.
8. Giovanini AF, Grossi JR, Gonzaga CC, Zielak JC, Gohringer I, Vieira JD *et al.* Leukocyte-platelet-rich plasma (L-PRP) induces an abnormal histophenotype in craniofacial bone repair associated with changes in the immunopositivity of the hematopoietic clusters of differentiation, osteoproteins, and TGF-beta1. *Clin Implant Dent Relat Res.* 2014,16(2):259-72.
9. Gresele P, Falcinelli E, Loffredo F, Cimmino G, Corazzi T, Forte L *et al.* Platelets release matrix metalloproteinase-2 in the coronary circulation of patients with acute coronary syndromes: possible role in sustained platelet activation. *Eur Heart J.* 2011;32:316-25.
10. Intini G. The use of platelet-rich plasma in bone reconstruction therapy. *Biomaterials.* 2009;30:4956-66.
11. Krieg T, Abraham D, Lafyatis R. Fibrosis in connective tissue disease: the role of the myofibroblast and fibroblast-epithelial cell interactions. *Arthritis Res Ther.* 2007;9 Suppl 2:S4.
12. Levi E, Fridman R, Miao HQ, Ma YS, Yayon A, Vlodyavsky I. Matrix metalloproteinase 2 releases active soluble ectodomain of fibroblast growth factor receptor 1. *Proc Natl Acad Sci USA.* 1996;93:7069-74.

13. Marx RE. Platelet-rich plasma: evidence to support its use. *J Oral Maxillofac Surg.* 2004;62:489-96.
14. Massague J, Gomis RR. The logic of TGFbeta signaling. *FEBS Lett.* 2006;580:2811-20.
15. Monnet E, Fauvel-Lafeve F. A new platelet receptor specific to type III collagen. Type III collagen-binding protein. *J Biol Chem.* 2000;275:10912-7.
16. Mooren RE, Hendriks EJ, van den Beucken JJ, Merkx MA, Meijer GJ, Jansen JA et al. The effect of platelet-rich plasma in vitro on primary cells: rat osteoblast-like cells and human endothelial cells. *Tissue Eng Part A.* 2010;16:3159-72.
17. Mosig RA, Dowling O, DiFeo A, Ramirez MC, Parker IC, Abe E et al. Loss of MMP-2 disrupts skeletal and craniofacial development and results in decreased bone mineralization, joint erosion and defects in osteoblast and osteoclast growth. *Hum Mol Genet.* 2007;16:1113-23.
- 18 Oliveira Filho MA, Nassif PA, Malafaia O, Ribas Filho JM, Ribas CA, Camacho AC et al. Effects of a highly concentrated platelet-rich plasma on the bone repair using non-critical defects in the calvaria of rabbits. *Acta Cir Bras.* 2010;25:28-33.
19. Ogawa K, Chen F, Kuang C, Chen Y. Suppression of matrix metalloproteinase-9 transcription by transforming growth factor-beta is mediated by a nuclear factor-kappaB site. *Biochem J.* 2004;381:413-22.
20. Risinger Jr. GM, Updike DL, Bullen EC, Tomasek JJ, Howard EW. TGF-beta suppresses the upregulation of MMP-2 by vascular smooth muscle cells in response to PDGF-BB. *Am J Physiol Cell Physiol.* 2010;298:C191-201.
21. Thiolloy S, Edwards JR, Fingleton B, Rifkin DB, Matrisian LM, Lynch CC. An osteoblast-derived proteinase controls tumor cell survival via TGF-beta activation in the bone microenvironment. *PLoS One.* 2012;7:e29862.
22. Tzaphlidou M. The role of collagen in bone structure: an image processing approach. *Micron.* 2005;36:593-601.